Application of Residual Correction Method on Hyperbolic Thermoelastic Response of Hollow Spherical Medium in Rapid Transient Heat Conduction

Po-Jen Su, Huann-Ming Chou

Abstract—In this article, we used the residual correction method to deal with transient thermoelastic problems with a hollow spherical region when the continuum medium possesses spherically isotropic thermoelastic properties. Based on linear thermoelastic theory, the equations of hyperbolic heat conduction and thermoelastic motion were combined to establish the thermoelastic dynamic model with consideration of the deformation acceleration effect and non-Fourier effect under the condition of transient thermal shock. The approximate solutions of temperature and displacement distributions are obtained using the residual correction method based on the maximum principle in combination with the finite difference method, making it easier and faster to obtain upper and lower approximations of exact solutions. The proposed method is found to be an effective numerical method with satisfactory accuracy. Moreover, the result shows that the effect of transient thermal shock induced by deformation acceleration is enhanced by non-Fourier heat conduction with increased peak stress. The influence on the stress increases with the thermal relaxation time.

Keywords—Maximum principle, non-Fourier heat conduction, residual correction method, thermo-elastic response.

I. INTRODUCTION

DUE to the extensive applications of the ultra-short pulse laser heating and the rapid metal solidification technology used in the material processing, analysis for the thermoelastic response in the solid is of considerable practical importance in engineering sciences. Theories of thermoelasticity are frequently used in a variety of engineering applications to deal with advanced engineering design problems for structures under thermal shock loads [1]-[3]. The conventional theory of thermo-elasticity introduced by Biot [4] is based on the Fourier's heat conduction law, which means that thermal disturbances propagate with infinite speed. However, this phenomenon of heat conduction is not in accordance with some new experimental results for the case involving extremely short transient or high heat flux [5], [6]. To eliminate the paradox of an infinite thermal wave speed and overcome the unacceptable predictions of conventional theory, [7] and [8] proposed the concept of the hyperbolic nature involving finite speed of thermal disturbance, known as the second sound. Chester [9]

P.J. Su is with the Metal Industries Research & Development Centre, Kaohsiung, 811 Taiwan, ROC (e-mail:superman0524@gmail.com).
H.M. Chou is with the Mechanical Engineering Department, Kun Shan University, Tainan, 701 Taiwan, ROC (phone: +886-6-2727175 Ext 260; fax:+886-6-2050063; e-mail:hmchou@mail.ksu.edu.tw).

discussed the possible existence of second sound in solids and provided some support for the contention that the second sound must exist in any solid. Numerous investigators have attempted to address unacceptable predictions produced by the conventional theory based on the general notion of relaxing the heat flux in the classical Fourier heat conduction equation by introducing one or more relaxation times, which are hence referred to as generalized thermo-elastic theories. In contrast to classical thermoelastic models in which the temperature disturbances are assumed to propagate at infinite speeds, modified theories involving non-Fourier heat conduction based on the general notion of relaxing the heat flux in the classical theory have been proposed to account for the finite speeds of thermal wave propagation and thermally-induced stress wave propagation. For instance, [10] and [11] independently postulated a constitutive relation between the heat flux vector ($\mathbf{q}$) and temperature gradient (∇T) in solids, the so-called CV wave model, as $\mathbf{q} + \tau_q \left(\partial \mathbf{q} / \partial t \right) = -k \nabla T$. τ_q indicates the observed time-lag, that is so-called thermal relaxation time. This equation can be used to account for the finite speed of heat. Coupling the CV-model to the energy conservation equation yields a hyperbolic equation, thereby introducing a non-Fourier effect.

The conventional thermoelastic theory involves the energy conservation equation based on the Fourier heat conduction law and the motion equation. Since the energy conservation equation takes a parabolic form and the equation of motion in terms of displacement within the infinitesimal deformation assumption is hyperbolic, the conventional thermo-elasticity includes a mixed parabolic-hyperbolic system. In contrast, the energy conservation equation considering non-Fourier heat conduction together with the motion equation turns out to be a hyperbolic-hyperbolic system, also known as hyperbolic thermo-elasticity. The energy conservation equation in the hyperbolic form for the non-Fourier heat conduction law can be reduced to the classical form with the parabolic equation when the relaxation time approaches to zero, thus this form of thermo-elasticity is also called as generalized thermoelasticity. Comprehensive literature surveys of hyperbolic thermoelasticity can be found in reviews by [12].

Since theoretical [13]-[15] and experimental studies support the finiteness of heat propagation speeds [16], [17], many investigations for thermoelastic problems were carried out

based on these generalized theories. With the development of transient heating technologies such as ultra-short and high energy density laser applications to enhance the properties of material surfaces, increased attention has focused on rapid heating combined with mechanical behavior. Classical thermo-elasticity has been found to be sufficient for general engineering applications, while modified thermo-elasticity based on non-Fourier heat conduction is more suitable for describing real transient heating [18].

Many studies have examined thermoelastic problems. Tanigawa et al. [19] analyzed transient thermal stress problems of solid and hollow spheres with spherically isotropic properties, noting the time-dependent variations of the thermal stress distributions caused by the variation of the thermo-elastic compliance constants. Hetnarski and Ignaczak [20] studied the response of semi-space to a short laser pulse in the context of generalized thermoelasticity. Lee [21] found the numerical solution of quasi-static coupled thermo-elastic problems for multilayered spheres by using the Laplace transform and matrix similarity transformation. The established computational procedures are capable of solving the generalized thermoelastic problem of multilayered spheres. Yu et al. [22] studied hyperbolic thermoelasticity due to pulsed heat input by the finite element method. They found the heat wave and elastic wave travel in the medium at a finite velocity and are reflected at the end of the rod.

In realistic engineering applications and scientific research, finding exact solutions for various governing equations is only possible in a very limited number of cases. It is usually difficult to find exact solutions for complex geometric shapes under the given initial and boundary conditions, to say nothing of involving nonlinear equations and/or non-homogeneous boundary conditions. Given this difficulty in obtaining analytic solutions for such complex geometric shapes with non-homogeneous boundary conditions, it is only possible to find their approximate solutions through certain numerical schemes to obtain approximate solutions and error ranges. One such scheme is the Residual Correction Method.

Previous studies have verified that the error margin between approximate and exact solutions usually decreases as the number of grid points or approximate functions increases, but this requires more calculation time and memory space. Nevertheless, it is still impossible to completely determine the accuracy of the approximate solution. Protter [23] proposed the concept of the maximum principle which explains the relationship between the solution and the residual of a differential equation and can be used to find the upper and lower approximate solutions of the exact solutions of some differential equations. However, until recently this concept had not been broadly applied in numerical methods. Applying this approach involves a programming problem of mathematical inequalities that requires time-consuming calculations. In recent years, some investigators have made attempts to simplify the calculating procedure. Lee et al. [24] successfully used genetic algorithms to apply simplified equations reliant on trial functions to handle programming problems generated in the optimization process. Su and Chen [25] extended previous

studies for non-Fourier heat conduction with the time-dependence boundary condition. Their study showed that incorporating the residual correction method into the nonlinear iterative procedure of the finite difference can make it easier and faster to obtain approximate solutions.

The main object of this article is to study the distributions of temperature, displacement and thermo-elastic stresses for an isotropic, homogeneous sphere due to thermal shock (i.e., sudden temperature change) on the spherical surface. The study uses the residual correction method based on maximum principles in differential equations, which is quite effective for obtaining the solution for distribution of temperature and displacement. Thermal stress is then solved. The advantage of this method lies in its capacity to restrict the exact solution within a known region, and thus obtain upper and lower approximate solutions. It can be used to estimate the range of the maximum possible error between the approximate solution and the exact solution, avoiding a blind increase of calculation grid points to obtain more accurate approximate solutions.

II. MATHEMATICAL PRELIMINARIES

The maximum principle of the differential equation is used as the main concept to form the complete structure in this study. Based on this, the upper and lower approximate solutions of the exact solution can be obtained. Analyzing the error according to the mean value of the upper and lower approximate solutions can effectively deal with the defects resulting from increasing the numbers of grids or approximate functions when using traditional numerical methods. This methodology can significantly reduce computing time, save memory, and promote numerical accuracy, and is expected to provide high academic value and practicability for future numerical research.

A. Maximum Principle for Differential Equations

The maximum principle for differential equations is a generalization of basic problems in calculus to describe a continuously differentiable function as having its maximum value at one endpoint of an interval if it satisfies the inequality $f''(x) > 0$ on the interval. That is to say, if a function satisfies a differential inequality in a domain and obtains its maximum value on the boundaries of the domain, we can say that the differential equation satisfies the maximum principle for differential equations with monotonicity. The approach is based on the concept of the maximum principle to build up the residual of differential equations and thus obtain the upper and lower approximate solutions. At first, assume a differential equation in the form below:

$$R_{\tilde{\theta}}(x) = F(x, \tilde{u}, \tilde{u}_x, \tilde{u}_{xx}) - f(x) \text{ in } D \tag{1}$$

Boundary conditions satisfy

$$R_{\tilde{\theta}}(x) = g(x) - \tilde{\theta}(x) \text{ on } \partial D \tag{2}$$

where the function $R_{\tilde{\theta}}(x)$ is known as the residual value function of the approximate function $\tilde{\theta}(x)$ of the differential equation in the domain D or on the boundaries ∂D. Assuming that the approximate solutions are defined in the calculation domain and are continuous to second derivatives, if

$$\frac{\partial R}{\partial \theta} \leq 0 \text{ in } D \tag{3}$$

then, if and only if the following relationship between the residual relation and approximate functions holds true

$$R_{\tilde{\theta}}(x) \geq R_{\theta}(x) = 0 \geq R_{\hat{\theta}}(x) \text{ on } D \cup \partial D \tag{4}$$

the approximate solutions will have the following relation with the exact solution:

$$\tilde{\theta}(x) \leq \theta(x) \leq \hat{\theta}(x) \text{ on } D \cup \partial D \tag{5}$$

where $\tilde{\theta}(x)$ and $\hat{\theta}(x)$ are respectively known as the lower and upper approximate solutions of the exact solution $\theta(x)$. A differential equation with such relations is considered monotonic.

B. Residual Correction Steps

Use the finite difference method to discretize and reformulate the residual relation into:

$$R_{r,i,j,k}(t,x,y,z) = -\left(L[\theta]_{r,i,j,k}^{n+1} + N[\theta]_{r,i,j,k}^{n} \right) + f_{r,i,j,k} \tag{6}$$

where L is the linear operator and N is the nonlinear operator, the superscript n is the number of iterations, and the subscript r,i,j,k is the serial number of the grid points after discretizing. Then, transfer the expression into an iterative equation with residual correction to avoid complex calculations:

$$-\left(L[\theta]_{r,i,j,k}^{n+1} + N[\theta]_{r,i,j,k}^{n} \right) + f_{r,i,j,k}$$
$$= \frac{\max}{\min}(\Delta R_{r,i,j,k}^{n}(t,x,y,z)) \tag{7}$$

where $\Delta R_{r,i,j,k}^{n}(t,x,y,z)$ indicates the residual distribution function of the last calculation results on adjacent subintervals of grid points. It can be expanded as follows using the Taylor series at the grid points:

$$\Delta R_{r,i,j,k}(t,x,y,z) = \sum_{s=1}^{\infty}\sum_{p=1}^{\infty}\sum_{q=1}^{\infty}\sum_{l=1}^{\infty} \frac{\partial R_{r,i,j,k}(t,x,y,z)}{\partial t^s \partial x^p \partial y^q \partial z^r}$$
$$\frac{(t-t_r)^s (x-x_i)^p (y-y_j)^q (z-z_k)^l}{s!p!q!r!} \tag{8}$$

$(t_r - \Delta t) \leq t \leq (t_r)$, $(x_i - \Delta x) \leq x \leq (x_i + \Delta x)$,

$(y_j - \Delta y) \leq y \leq (y_j + \Delta y)$, $(z_k - \Delta z) \leq z \leq (z_k + \Delta z)$

Finally, the residual values on the adjacent subintervals of the grids can be ensured to be all positive or all negative by the residual values at the calculation grids which are corrected by identifying the maximum and minimum of residual values on these intervals.

The convergence criterion applied in the present study is the relative error convergence as defined by:

$$E_{\theta} = \left| \frac{\tilde{\theta}_i^{n+1} - \tilde{\theta}_i^{n}}{\tilde{\theta}_i^{n}} \right| \leq \varepsilon, \quad i = 0,1,\cdots,N_i \tag{9}$$

III. MODEL DESCRIPTION

This study deal with the one-dimensional thermoelastic problems of a hollow sphere, with symmetry under the following assumptions:
(1). Material is assumed to be isotropic and homogeneous, and to have constant thermal properties.
(2). Deformation and strain satisfy Hooke's law.
(3). All physical quantities are assumed to be functions of the radial coordinate and time only.
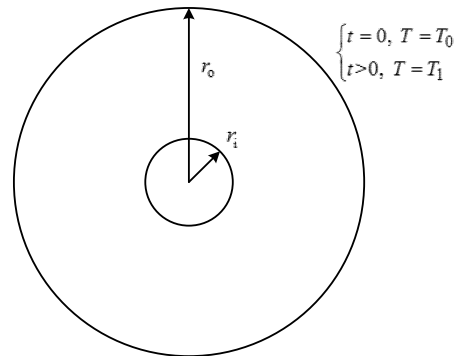(4). The medium is initially undisturbed and traction free on surface, without body forces or internal heat sources.

Fig. 1 Computation domain

Consider a hollow spherical medium with the inner radius r_i and outer radius r_o, as shown in Fig. 1. The body is at rest and with a uniform initial temperature, $T = T_0$. Expose a thermal shock to the body by changing the temperature on the entire boundary of spherical surface from $T = T_0$ to $T = T_1$. Thus the boundary of the spherical surface remains steady at this temperature and allows the boundary to move without any restriction.

In this study (due to spherical symmetry), the displacement and temperature are assumed to be functions of space, r and time, t only. The arising displacements in the spherical coordinate (r, θ, ϕ) can be expressed as:

$$u_r = u_r(r,t), \ u_{\theta} = 0, \ u_{\phi} = 0 \tag{10}$$

Considering the strain–displacement relations, the strain components can be written as:

$$\varepsilon_{rr} = \frac{\partial u_r}{\partial r}, \quad \varepsilon_{\theta\theta} = \varepsilon_{\phi\phi} = \frac{u_r}{r}, \quad \varepsilon_{r\theta} = \varepsilon_{r\phi} = \varepsilon_{\theta\phi} = 0 \tag{11}$$

The stress-displacement relations are

$$\sigma_{rr} = \frac{E}{1-2v}\left[\frac{1-v}{1+v}\frac{\partial u_r(r,t)}{\partial r} + \frac{2v}{1+v}\frac{u_r(r,t)}{r} - \alpha\left(T(r,t)-T_0\right)\right] \tag{12}$$

$$\sigma_{\theta\theta} = \sigma_{\phi\phi} = \frac{E}{1-2v}\left[\frac{v}{1+v}\frac{\partial u_r(r,t)}{\partial r} + \frac{1}{1+v}\frac{u_r(r,t)}{r} - \alpha\left(T(r,t)-T_0\right)\right] \tag{13}$$

where σ_{rr} and $\sigma_{\theta\theta}$ are stress components of r and θ direction, respectively. E is Young's Modulus, v is Poisson's ratios, α is the coefficients of linear thermal expansion. $u_r(r,t)$ and $T(r,t)$ are respectively the distributions of media of rising displacement and temperature.

Based on the non-Fourier heat conduction and linear thermoelastic theory, the governing equations of temperature and displacement of the sphere are formulated as,

$$\frac{\partial^2 T(r,t)}{\partial r^2} + \frac{2}{r}\frac{\partial T(r,t)}{\partial r} = \frac{1}{a}\frac{\partial T(r,t)}{\partial t} + \frac{\tau_q}{a}\frac{\partial^2 T(r,t)}{\partial t^2} \tag{14}$$

$$\frac{\partial^2 u_r(r,t)}{\partial r^2} + \frac{2}{r}\frac{\partial u_r(r,t)}{\partial r} - \frac{2}{r^2}u_r(r,t) - \frac{1}{V_E^2}\frac{\partial^2 u_r(r,t)}{\partial t^2} = \alpha\frac{1+v}{1-v}\frac{\partial T(r,t)}{\partial r} \tag{15}$$

where $V_E = \sqrt{\frac{(1-v)E}{(1+v)(1-2v)\rho}}$ is the speed of the thermal-elastic wave, and $a = k/\rho c$ is the thermal diffusivity.

The initial and boundary conditions described above are expressed as

$$t = 0: \quad T(r,t) = T_0, \quad \frac{\partial T(r,t)}{\partial t} = 0; \quad u(r,t) = \frac{\partial u(r,t)}{\partial t} = 0 \tag{16}$$

$$r = r_o: \quad T(b,t) = T_1; \quad \sigma_r(r,t) = 0 \tag{17}$$

$$r = r_i: \quad \frac{\partial T(r,t)}{\partial r} = 0; \quad \sigma_r(r,t) = 0 \tag{18}$$

For the convenience of subsequent analysis, the following dimensionless quantities are defined:

$$\eta = \frac{V_E r}{a}; \quad \xi = \frac{V_E^2 t}{a}; \quad \xi_\tau = \frac{V_E^2 \tau_q}{a}; \quad \Theta = \frac{T-T_0}{T_1-T_0};$$

$$\Psi = \frac{1-v}{(1+v)\alpha(T_1-T_0)}\frac{V_E u_r}{a};$$

$$\Omega_i = \frac{1-2v}{\alpha E(T_1-T_0)}\sigma_i, \quad (i = r,\theta,\phi). \tag{19}$$

Equations (14) and (15) are expressed in terms of the above dimensionless variables as

$$\frac{\partial^2 \Theta}{\partial \eta^2} + \frac{2}{\eta}\frac{\partial \Theta}{\partial \eta} = \xi_\tau\frac{\partial^2 \Theta}{\partial \xi^2} + \frac{\partial \Theta}{\partial \xi} \tag{20}$$

and

$$\frac{\partial^2 \Psi}{\partial \eta^2} + \frac{2}{\eta}\frac{\partial \Psi}{\partial \eta} - \frac{2}{\eta^2}\Psi - \frac{\partial^2 \Psi}{\partial \xi^2} = \frac{\partial \Theta}{\partial \eta} \tag{21}$$

The dimensionless initial and boundary conditions and stress are represented as

$$\xi = 0: \quad \Theta(\eta,\xi) = \frac{\partial \Theta(\eta,\xi)}{\partial \xi} = 0; \quad \Psi(\eta,\xi) = \frac{\partial \Psi(\eta,\xi)}{\partial \xi} = 0 \tag{22}$$

$$\eta = 0: \quad \frac{\partial \Theta(\eta,\xi)}{\partial \eta} = 0; \quad \Psi(\eta,\xi) = 0 \tag{23}$$

$$\eta = 1: \quad \Theta(\eta,\xi) = 1; \quad \Omega_r(\eta,\xi) = 0 \tag{24}$$

$$\Omega_r = \frac{\partial \Psi(\eta,\xi)}{\partial \eta} + \frac{2v}{1-v}\frac{\Psi(\eta,\xi)}{\eta} - \Theta(\eta,\xi) \tag{25}$$

$$\Omega_\theta = \Omega_\phi = \frac{v}{1-v}\frac{\partial \Psi(\eta,\xi)}{\partial \eta} + \frac{1}{1-v}\frac{\Psi(\eta,\xi)}{\eta} - \Theta(\eta,\xi) \tag{26}$$

To analyze the error of approximate solutions of temperature and displacement, the residual correction relations are respectively established for (20) and (21) first, in the form of

$$R_1 = \frac{\partial^2 \Theta(\eta,\xi)}{\partial \eta^2} + \frac{2}{\eta}\frac{\partial \Theta(\eta,\xi)}{\partial \eta} - \xi_\tau\frac{\partial^2 \Theta(\eta,\xi)}{\partial \xi^2} - \frac{\partial \Theta(\eta,\xi)}{\partial \xi} \tag{27}$$

$$R_2 = \frac{\partial^2 \Psi(\eta,\xi)}{\partial \eta^2} + \frac{2}{\eta}\frac{\partial \Psi(\eta,\xi)}{\partial \eta} - \frac{2}{\eta^2}\Psi(\eta,\xi) - \frac{\partial^2 \Psi(\eta,\xi)}{\partial \xi^2} - \frac{\partial \Theta(\eta,\xi)}{\partial \eta} \tag{28}$$

Before continuing the calculation steps, apply the above-mentioned maximum principle to determine whether the monotonic characteristic is present in (27) and (28).

$$\frac{\partial R_1}{\partial \Theta} = \frac{\partial}{\partial \Theta}\left[\frac{\partial^2 \Theta(\eta,\xi)}{\partial \eta^2} + \frac{2}{\eta}\frac{\partial \Theta(\eta,\xi)}{\partial \eta} - \xi_\tau\frac{\partial^2 \Theta(\eta,\xi)}{\partial \xi^2} - \frac{\partial \Theta(\eta,\xi)}{\partial \xi}\right] = 0 \tag{29}$$

$$\frac{\partial R_2}{\partial \Psi} = \frac{\partial}{\partial \Psi}\left[\frac{\partial^2 \Psi(\eta,\xi)}{\partial \eta^2} + \frac{2}{\eta}\frac{\partial \Psi(\eta,\xi)}{\partial \eta} - \frac{2}{\eta^2}\Psi(\eta,\xi)\right.$$
$$\left. - \frac{\partial^2 \Psi(\eta,\xi)}{\partial \xi^2} - \frac{\partial \Theta(\eta,\xi)}{\partial \eta}\right] = -\frac{2}{\eta^2} \qquad (30)$$

If the maximum principle is satisfied, the required condition is:

$$\frac{\partial R_1}{\partial \Theta} \le 0 \quad \text{and} \quad \frac{\partial R_2}{\partial \Psi} \le 0. \qquad (31)$$

Because the value of η in (30) is positive, (31) holds. Therefore, the monotonicity exits. Subsequently, the residual correction method is used in combination with the finite difference method of the implicit scheme to discretize (20) and (21). To add the residual correction value at every calculation grid points, the iteration relations of temperature and displacement will be generated as

$$\left(\frac{1}{(\Delta\eta)^2} - \frac{1}{\eta_i \cdot \Delta\eta}\right)\Theta_{i-1}^{n+1} + \left(-\frac{2}{(\Delta\eta)^2} - \frac{1}{2\cdot\Delta\xi} - \frac{\xi_\tau}{(\Delta\xi)^2}\right)\Theta_i^{n+1}$$
$$+ \left(\frac{1}{(\Delta\eta)^2} + \frac{1}{\eta_i \cdot \Delta\eta}\right)\Theta_{i+1}^{n+1} = \left(-\frac{2\xi_\tau}{(\Delta\xi)^2}\right)\Theta_i^n + \left(\frac{\xi_\tau}{(\Delta\xi)^2} - \frac{1}{2\Delta t}\right)\Theta_i^{n-1} \quad (32)$$
$$- \frac{\text{Min}}{\text{Max}}\left(0, -R_\xi^n \Delta\xi\right) - \frac{\text{Min}}{\text{Max}}\left(R_\eta^n \Delta x, -R_\eta^n \Delta\eta\right)$$

$$\left(\frac{1}{(\Delta\eta)^2} - \frac{1}{\eta_i \cdot \Delta\eta}\right)\Psi_{i-1}^{n+1} + \left(-\frac{2}{(\Delta\eta)^2} - \frac{2}{\eta_i^2} - \frac{1}{(\Delta\xi)^2}\right)\Psi_i^{n+1}$$
$$+ \left(\frac{1}{(\Delta\eta)^2} + \frac{1}{\eta_i \cdot \Delta\eta}\right)\Psi_{i+1}^{n+1} = -\frac{2}{(\Delta t)^2}\Psi_i^n + \frac{1}{(\Delta\xi)^2}\Psi_i^{n-1} \qquad (33)$$
$$+ \frac{1}{2\Delta\eta}\left[\Theta_{i+1}^{n+1} - \Theta_{i-1}^{n+1}\right] - \frac{\text{Min}}{\text{Max}}\left(0, -R_\xi^n \Delta\xi\right) - \frac{\text{Min}}{\text{Max}}\left(R_\eta^n \Delta\eta, -R_\eta^n \Delta\eta\right)$$

Next, the central finite difference method is used discretize the initial and boundary conditions (22)~(24), as:

$$\Theta_i^{n=0} = 0, \ \Theta_i^{n+1} = \Theta_i^{n-1}; \ \Psi_i^{n=0} = 0; \ \Psi_i^{n+1} = \Psi_i^{n-1} \qquad (34)$$

$$\Theta_{i+1}^n = \Theta_{i-1}^n, \ \Psi_0^n = 0 \qquad (35)$$

$$\Theta_{Ni}^n = 1, \ \Psi_{i+1}^n = \Psi_{i-1}^n + 2\Delta\eta\left(-\frac{2\nu}{1-\nu}\frac{\Psi_{Ni}^n}{\eta_{Ni}} + \Theta_{Ni}^n\right) \qquad (36)$$

The selected residual correction value at each grid point is either the minimum or the maximum in this grid to ensure $R_{1\Theta}(\eta,\xi) \ge 0$ or $R_{1\Theta}(\eta,\xi) \le 0$; $R_{2\Psi}(\eta,\xi) \ge 0$ or $R_{2\Psi}(\eta,\xi) \le 0$. For the above expressions, if two variables η and ξ of (27) and (28) are partially differentiated, and the differential terms of a higher order, $\Theta_{\eta\eta\eta}$, $\Theta_{\xi\xi\xi}$, $\Psi_{\eta\eta\eta}$, and $\Psi_{\xi\xi\xi}$ can be expressed as

$$R_{1\eta} = \left(-2\eta^{-2}\Theta_\eta + 2\eta^{-1}\Theta_{\eta\eta}\right) - \xi_\tau\Theta_{\eta\xi\xi} - \Theta_{\eta\xi} \qquad (37)$$

$$R_{1\xi} = \Theta_{\xi\eta\eta} + 2\eta^{-1}\Theta_{\xi\eta} - \Theta_{\xi\xi} \qquad (38)$$

$$R_{2\eta} = -4\eta^{-2}\Psi_\eta + 2\eta^{-1}\Psi_{\eta\eta} + 4\eta^{-3}\Psi - \Psi_{\eta\xi\xi} - \Theta_{\eta\eta} \qquad (39)$$

$$R_{2\xi} = \Psi_{\xi\eta\eta} + 2\eta^{-1}\Psi_{\xi\eta} - 2\eta^{-2}\Psi_\xi - \Theta_{\xi\eta} \qquad (40)$$

Finally, calculate iteratively to obtain numerical solutions when they meet the convergence criterion. Here, set the relative tolerant error ε as 10^{-8}. In the iterative process, the residual corrections are added together and the calculation is iterated until $\tilde{\Theta}^n$, $\tilde{\Theta}^{n+1}$, $\tilde{\Psi}^n$ and $\tilde{\Psi}^{n+1}$ satisfy the convergence criterion to find the approximate solutions of the upper and lower bounds.

IV. RESULTS AND DISCUSSION

To numerically assess the correctness of the residual correction method, we first conduct the grid convergence test. The number of grid points is crucial in the numerical analysis and has a significant impact on accuracy and efficiency. The distributions of dimensionless temperature and displacement for various numbers of grid points are illustrated in Figs. 2 and 3. Higher accuracy is obtained as the number of grid points increases. However, the discrepancy between N=400 and N=800 is not distinct and the mean solutions nearly overlap. The results indicate that the mean approximate solution can be acquired even with fewer grid points. Thus, as far as calculation efficiency is concerned, calculation could proceed with fewer grid points. Moreover, as shown in the figures, the upper approximate solutions are always distributed above the lower approximate solutions in the whole calculation domain. It is clear that the mean approximate solutions are always located between the upper and lower approximate solutions. The upper and lower approximate solutions gradually tend to approach each other as the number of grid points increases and always satisfy the requirement for monotonic residual relation.
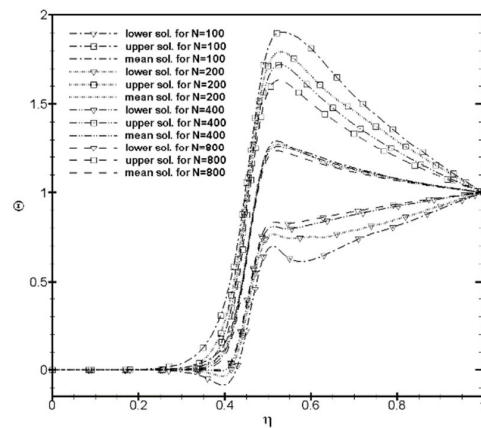

Fig. 2 Upper, lower and mean solutions of dimensionless temperature distributions for various grid number values. ($\xi = 0.3$, $\xi_\tau = 0.3$)

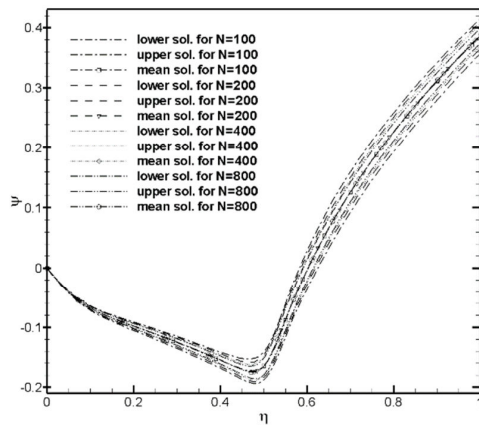Fig. 3 Upper, lower and mean solutions for dimensionless displacement variation distributions for various grid number values ($\xi = 0.5$, $\xi_\tau = 0.25$)
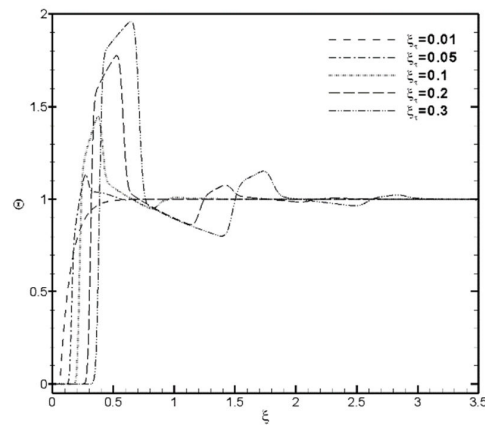

Fig. 4 Dimensionless temperature distributions versus time for various dimensionless relaxation times ($\eta = 0.3$)

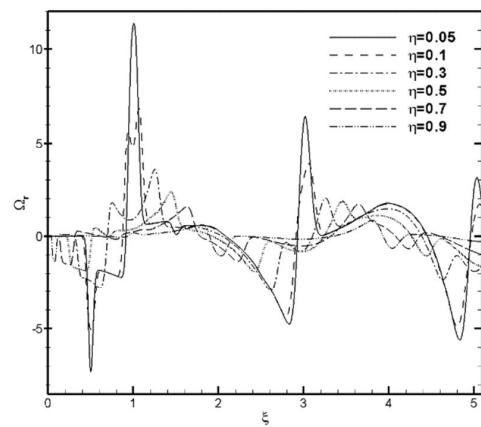Fig. 5 Curves of dimensionless radial stress versus time at different positions ($\xi_\tau = 0.01$)

Fig. 4 shows the dimensionless temperature profiles as time increases at $\eta = 0.3$. Higher and wavy shaped temperature patterns are seen as the relaxation time increased. This phenomenon is due to the nature of the hyperbolic heat conduction equation, which induces the thermal wave and leads to a discontinuous temperature response. According to the formula for the speed of a dimensionless thermal wave, $\tilde{v} = 1/\sqrt{\xi_\tau}$. While the thermal relaxation time is extremely small ($\xi_\tau = 0.01$ in this case), the propagation speed of thermal disturbance passes forward rapidly. The curve indicates a continuous temperature distribution inside the sphere. This heat transfer process can be considered to be a Fourier heat conduction. As thermal relaxation time increases, the speed of thermal disturbance decays rapidly. The lagging effect between the distribution of heat flux and temperature causes the temperature distribution inside the sphere to present a step distribution and forms a temperature gradient with a large amplitude. That is to say, the effect of non-Fourier heat conduction induces thermal waves and leads to a discontinuous temperature response resulting in a finite speed of propagation of the thermal waves.

Figs. 5 and 6 show the curve of the dimensionless radial and circumferential stress varied at different position versus time for the given dimensionless thermal relaxation time, $\xi_\tau = 0.01$. When the spherical surface is subjected to a thermal shock, the thermal disturbance induces the thermo-elastic wave propagation forward in the form of a wave. In the meantime, the elastic wave arriving at the outer spherical surface is reflected, and the reflected wave continues to propagate to the interior of the sphere. Superimposing the incident and reflected wave, the periodic stress field distribution inside the sphere presents an alternating tensile and compressive stress. The closer to the center of the sphere, the greater the stress peak gets.

Figs. 7 and 8 respectively indicate the influence of the dimensionless thermal relaxation time on the variation of radial and circumferential stress versus time. The temperature presents a continuous distribution in the interior of the sphere when the thermal relaxation time was small. Thus, at this time, the stress deformation within the sphere is mainly determined by the acceleration generated by the dynamic thermal stresses. The stress peak is relatively small. As the dimensionless relaxation time ξ_τ increases, the speed of thermal disturbance decays rapidly. Due to the effect of non-Fourier heat conduction result to great temperature gradient, it is clearly seen in Fig. 4. Under the effect of the great temperature gradient, various points along the sphere's periphery are squeezed together by the effects of thermal expansion, thus creating a larger peak stress. When the speed of the propagated thermal wave is finite the delay generates a non-Fourier heat conduction effect which increases the impact of the dynamic shock as the speed of the material deformation accelerates. This leads to the formation of large amplitude stress distributions within the sphere.
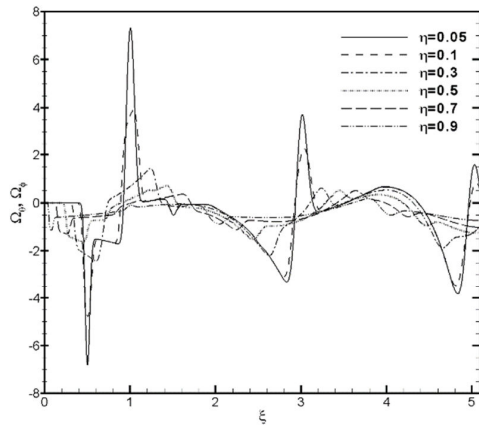
Fig. 6 Curves of dimensionless circumferential stress versus time at different positions ($\xi_\tau = 0.01$)
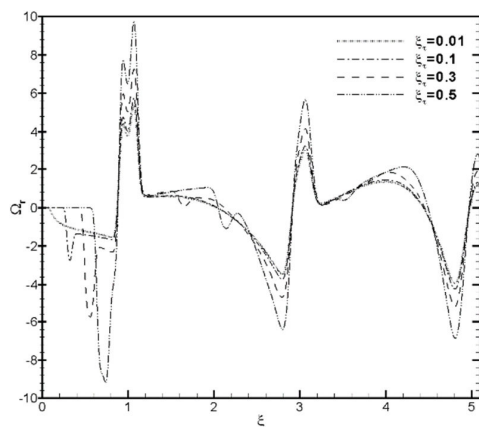

Fig. 7 Curves of dimensionless radial stress versus time for different dimensionless thermal relaxation times ($\eta = 0.1$)
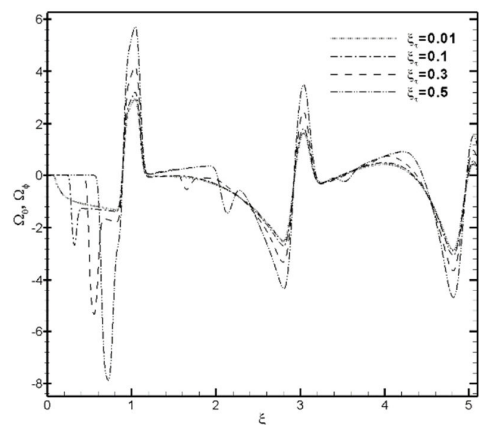

Fig. 8 Curves of dimensionless circumferential stress versus time for different dimensionless thermal relaxation times ($\eta = 0.1$)

V. CONCLUSIONS

The residual correction method based on the maximum principle in combination with the finite difference method was verified for solving the dynamic stress response in a solid sphere under thermal shock. The proposed residual correction method is found to effectively identify upper and lower approximate solutions. The residual correction values at every grid point can be handled simultaneously in the solution process without requiring additional iterations. In addition to producing mean approximate solutions with acceptable numerical accuracy, the method allows us to estimate the range of maximum possible error between the approximate and exact solutions and to avoid a blind increase in the calculation grid points to obtain more accurate approximate solutions.

Based on the non-Fourier heat conduction effects under rapid heating, the mathematical models about temperature fields, displacement fields and stress fields of the spherical material under thermal shock are established by the hyperbolic heat conduction equation and the thermo-elastic governing equation. It is shown that the distribution of thermal stress filed caused by the lagging phenomena of heat flux is different from the traditional distribution, and the stress peak is also higher than the result of traditional heat conduction.

From the calculated results we can observe that there is a concentration of dynamic stress at the center of a solid sphere and periodical oscillation due to the reflection of stress waves at the sphere's external boundary. The simulation shows the effect of the non-Fourier heat conduction causes the speed of the thermal disturbance to decay rapidly as the dimensionless relaxation time increases. Under the effect of superposition of the incident and reflected waves, the periodic stress field distribution inside the sphere presents alternating tensile and compressive stresses. Closer center of the sphere, the stress peaks increase. Moreover, the front of the elastic wave in the center of the sphere is continuously pooled and collided causing the formation of the stress concentration at the center of the sphere when the thermal-elastic wave propagates to the interior of the sphere. Peak stress increases rapidly with the thermal relaxation time.

REFERENCES

[1] Forgac, J.M. and Angus, J.C., "Solidification of metal spheres," Metallurgical Transactions, Vol. 12, No. 2, pp 413-416, 1981.

[2] Hata, T., "Thermal shock in a hollow sphere caused by rapid uniform heating," ASME Journal of Applied Mechanics, Vol. 58, pp. 64-69, 1991.

[3] Tang, D.W. and Araki, N., "Non-Fourier heat conduction in a finite medium under periodic surface thermal disturbance," International Journal of Heat and Mass Transfer, Vol. 39, No. 8, pp. 1585-1590, 1996.

[4] Biot, M.A., "Thermoelasticity and irreversible thermodynamics," Journal of Applied Physics, Vol. 27, No. 3, pp. 240-253, 1956.

[5] Peshkov, V., "Second sound in helium II," Journal of Physics, Vol. 8, pp. 381-386, 1944.

[6] Joseph, D.D. and Preziosi, L., "Heat waves," Reviews of Modern Physics, Vol.61, No. 1, pp. 41-73, 1989.

[7] Maxwell, J.C., "On the dynamic theory of gases," Philosophical Transactions of the Royal Society of London, Vol. 157, pp. 49-88 (1867).

[8] Nernst, W., "Die Theoretischen und Experimentellen Grundlagen des Neuen Warmesatzes," Knapp, Halle (1918).

[9] Chester, M., "Second sound in solids," Physical Review, Vol. 131, pp. 2013-2015, 1963.

[10] Cattaneo, C., "A form of heat conduction equation which eliminates the paradox of instantaneous propagation," Compte Rendus Acad. Sci., Vol. 247, pp. 431-433 (1958).

[11] Vernotte, P., "Some possible complications in the phenomena of thermal conduction," Compt. Rend. Acad. Sci. 252, pp. 2190-2191 (1961).

[12] Chandrasekharaiah, D.S., "Hyperbolic thermoelasticity, a review of recent literature," Applied Mechanics Reviews, Vol. 51, 705-729 (1998).

[13] Taitel, Y., "On the parabolic, hyperbolic and discrete formulation of the heat conduction equation, International Journal of Heat and Mass Transfer," Vol. 15, pp. 369-371 (1972).

[14] Frankel, J.I., Vick, B. and Ozisik, M.N., "Flux formulation of hyperbolic heat conduction," Journal of Applied Physics, Vol. 58, No. 9, pp. 3340-3345 (1985).

[15] Hong, B.S., Su, P.J., Chou, C.Y.; Hung, C.I., "Realization of non-Fourier phenomena in heat transfer with 2D transfer function," Applied Mathematical Modelling, Vol. 35, pp. 4031-4043 (2011).

[16] Kaminiski, W., "Hyperbolic heat conduction equation for materials with a nonhomogeneous inner structure," ASME Journal of Heat Transfer, Vol. 112, pp. 555-560 (1990).

[17] Mitra, K., Kumar, S., Vedavarz, A. and Moallemi, M.K., "Experimental evidence of hyperbolic heat conduction in processed meat," ASME Journal of heat transfer, Vol. 117, No. 3, pp. 568-573 (1995).

[18] Lord, H.W. and Shulman Y., "A generalized dynamical theory of thermoelasticity," Journal of the Mechanics and Physics of Solids, Vol. 15, No. 5, pp. 299-309 (1967).

[19] Tanigawa, Y., Takeuti, Y. and Ueshima, K., "Transient thermal stresses of solid and hollow spheres with spherically isotropic thermoelastic properties," Archive of applied mechanics, Vol. 54, pp. 259-267 (1984).

[20] Hetnarski, R.B. and Ignaczak, J., "Generalized Thermoelasticity: Response of semi-space to a short laser pulse," Journal of Thermal Stresses, Vol. 17, pp. 377-396 (1994).

[21] Lee, Z.Y., "Coupled problem of thermoelasticity for multilayered spheres with time-dependent boundary conditions," Journal of Marine Science and Technology, Vol. 12, No. 2, pp. 93-101 (2004).

[22] Yu, N., Imatani, S. and Inoue, T., "Title: Hyperbolic Thermoelastic Analysis due to Pulsed Heat Input by Numerical Simulation," JSME International Journal Series A, Vol. 49, No. 2, pp. 180-187 (2006).

[23] Proter, M.H. and Weinberger, H.F., "Maximum Principles in Differential Equations," Prentice-Hall (1967).

[24] Lee, Z.Y., Chen, C.K. and Hung, C.I., "Upper and lower bounds of the solution for an elliptic plate problem using a genetic algorithm," Acta Mechanica, Vol. 157, pp. 201-212 (2002).

[25] Su, P.J. and Chen, C.K., "Application of Residual Correction Method on non-Fourier Heat Transfer for Sphere with Time-Dependent Boundary Condition," CMES: Computer Modeling in Engineering & Science, Vol. 91, No. 2, pp. 135-151 (2013).